

Huge Magnetic Anisotropy in a Trigonal-Pyramidal Nickel(II) Complex

Silvia Gómez-Coca,^{*,†} Eduard Cremades,[†] Núria Aliaga-Alcalde,[‡] and Eliseo Ruiz^{*,†}

[†]Departament de Química Inorgànica and Institut de Recerca de Química Teòrica i Computacional, Universitat de Barcelona, Diagonal 645, E-08028 Barcelona, Spain

[‡]ICREA Researcher (Institució Catalana de Recerca i Estudis Avançats), Institut de Ciència de Materials de Barcelona (ICMAB-CSIC) Campus de la UAB, 08193 Bellaterra, Spain

Supporting Information

ABSTRACT: The work presented herein shows the experimental and theoretical studies of a mononuclear nickel(II) complex with the largest magnetic anisotropy ever reported. The zero-field-splitting D parameter, extracted from the fits of the magnetization and susceptibility measurements, shows a large value of -200 cm^{-1} , in agreement with the theoretical value of -244 cm^{-1} obtained with the CASPT2–RASSI method.

A single-molecule-magnet (SMM) retains magnetization because of the presence of an energy barrier that assists blocking of the reorientation of the magnetic moment. Such a barrier depends on the total spin of the ground state (S) and the zero-field-splitting (ZFS) axial parameter (D).¹ Interest in this family of complexes arises from their potential technological applications regarding data storage or quantum computing, even though the requirements for each purpose are not the same. Hence, for computing storage, two different well-defined states with obvious energy barriers and without (or with the minimum) quantum tunnelling of the magnetization (QTM) are needed. In contrast, for quantum computation, two states, $|0\rangle$ and $|1\rangle$ (or their combinations) are necessary to define a qubit.² Despite that, in both cases, the magnetic anisotropic parameters of the complex are crucial because D controls the barrier height and E , the ZFS rhombic parameter, is related to the QTM. Equation 1 shows the relationship between the ZFS parameters and elements of the diagonalized \mathbf{D} tensor.

$$D = D_{zz} - (D_{xx} + D_{yy})/2; \quad E = (D_{xx} - D_{yy})/2 \quad (1)$$

The first mononuclear SMM containing a 3d transition-metal center was reported by Long and co-workers³ in 2010. The system consisted of an iron(II) complex displaying a trigonal-pyramidal structure that retained the magnetization when an external direct-current (dc) field was applied. By that time, some of us also had published theoretical studies for trigonal-pyramidal iron(II) complexes.⁴ Showing that trigonal-pyramidal geometry (also called vacant trigonal-bipyramidal or trigonal-monopyramidal geometry) provides splitting of the d orbitals in the manner shown in Figure 1 [but for six electrons, in the case of iron(II) complexes, instead of eight as is shown]. Figure 1 shows that the degeneracy of the nonbonding orbitals is broken because of Jahn–Teller distortion, resulting in the existence of the first excited state very close in energy to the ground state. This affects

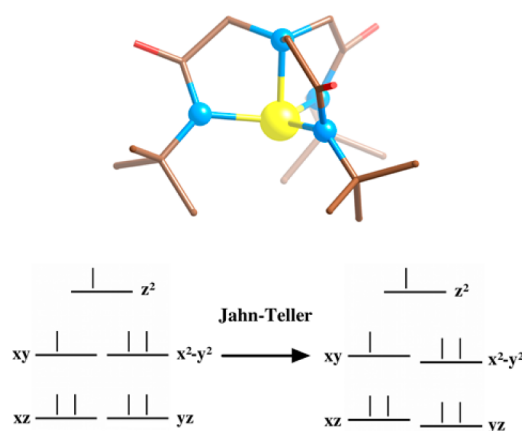


Figure 1. (Top) Molecular structure of the anion complex determined by single-crystal X-ray diffraction of **1**. Yellow, red, light blue, and brown represent nickel, oxygen, nitrogen, and carbon atoms, respectively. Hydrogen atoms have been omitted for clarity. (Bottom) Splitting of the d orbitals for a perfect trigonal-pyramidal coordination (left) and after Jahn–Teller distortion (right).

directly the magnitude of D , which is inversely proportional to the first excitation energy. Therefore, the closest the first excited state is to the ground state, the greatest the D values for these systems are.⁵ The dependence of D with the excitation energy can be extracted from the elements of the diagonalized \mathbf{D} tensor, which can be obtained from eq 2

$$D_{kl} = -\frac{\zeta_{\text{eff}}^2}{4S^2} \left[\sum_{i,p} \frac{\langle \varphi_i | l_k | \varphi_p \rangle \langle \varphi_p | l_l | \varphi_i \rangle}{\epsilon_p - \epsilon_i} - \sum_{p,a} \frac{\langle \varphi_i | l_k | \varphi_a \rangle \langle \varphi_a | l_l | \varphi_i \rangle}{\epsilon_a - \epsilon_p} \right] \quad (2)$$

where ζ_{eff} is the spin–orbital coupling constant, l_k is the k component of the angular momentum operator, and φ is a molecular orbital (with orbital energy ϵ) with the subindex i , p , or a to indicate double- and single-occupied or empty orbitals, respectively.

After the discovery of a trigonal-pyramidal iron(II) complex, the family of mononuclear SMM 3d transition-metal complexes has quickly grown with the addition of new iron(II) and cobalt(II) complexes with a variety of coordination geometries.

Received: September 16, 2013

Published: December 23, 2013



For iron(II) cations, the reported mononuclear SMMs have shown linear,⁶ trigonal-planar,⁷ trigonal-pyramidal,^{3,8} and unusual $6(S+1)^9$ distorted coordinations with negative D values between -6.2 and -51.4 cm^{-1} . For cobalt(II), published complexes with this behavior, either with negative or positive D values (found between -74 and 98 cm^{-1}), have tetrahedral,¹⁰ square-pyramidal,¹¹ trigonal-prismatic,^{5,12} octahedral,¹³ and trigonal-pyramidal⁵ distorted coordinations. On the other hand, nickel(II) complexes ($S = 1$) have also been studied during the last years because of the same appealing magnetic properties and because of the big D values that some of these complexes present.¹⁴ However, mononuclear nickel(II) systems do not behave as SMMs basically because of the existence of only three M_S states in the ground state and the strong coupling between their $M_S = \pm 1$, but they can present huge anisotropy, which can be employed for other purposes. Recently, different coordination modes such as tetrahedral,^{14a} octahedral,^{14b} pentagonal-bipyramidal,^{14c} and trigonal-bipyramidal^{14d} have been published, where the last one shows the biggest D reported until now with a value between -120 and -180 cm^{-1} .

Following the splitting of the d orbitals shown in Figure 1 for a d^8 transition metal with trigonal-pyramidal coordination, the degeneracy of the d_{xy} and $d_{x^2-y^2}$ orbitals is clear. This degeneracy will be broken because of Jahn–Teller distortion, giving again a first excited state very close to the ground state and, therefore, a large D parameter (see refs 15a and 15b for a detailed discussion of the Jahn–Teller effect involving an orbital doublet 3E ground state). The energy splitting between these two orbitals will increase depending on the structural distortions, resulting in a decrease of the D value. Thus, nickel(II) trigonal-pyramidal complexes with minor distortions are perfect candidates to study the magnetic anisotropy in 3d transition-metal complexes. A search in the Cambridge Structural Database,¹⁶ in combination with continuous-shape measurements,¹⁷ has provided us with a selected number of synthetic targets that showed the slightest distortions from the ideal shape. In this work, the chosen mononuclear nickel(II) complex was previously reported by Borovik and co-workers.¹⁸ The synthesis of $\text{K}\{\text{Ni}[\text{N}(\text{CH}_2\text{C}(\text{O})\text{NC}(\text{CH}_3)_3)_3]\}$ (**1** in Figure 1) was performed in a way similar to that of Borovik and co-workers but crystallizing with K^+ as the cation instead of tetraethylammonium. The tripodal ligand used confers the required rigidity, diminishing structural distortions. Continuous-shape measurement (S) for complex **1** gives a value of 0.317, confirming the small structural distortion ($S = 0$ corresponds to the ideal polyhedron).

Complex **1** was theoretically studied by first performing a CASSCF or CASPT2 calculation and later mixing the energy of these calculated states with the SO-RASSI approach (*MOLCAS* code).²⁰ We used an all-electron ANO-RCC basis set: nickel atoms (6s5p4d2f), nitrogen and oxygen (4s3p1d), carbon (3s2p), and hydrogen (2s) with an active space considering the eight d electrons of the nickel(II) centers and the five d orbitals. In a hypothetically nondistorted geometry, the ground state with degenerate d_{xy} and $d_{x^2-y^2}$ orbitals will correspond to a doubly degenerate 3E state. CASSCF calculation of the spin-free energies of **1** gives an energy difference between the ground state and the first excited state (also 3E term) of 814 cm^{-1} (942 cm^{-1} at the CASPT2 level). Such an energy difference can be attributed to the distortion induced in complex **1** by the Jahn–Teller effect because such states must be degenerate for the nondistorted structure. The inclusion of the spin–orbit coupling leads to six states (Table 1) because of the spin–orbit operator couples the $M_S = +1$ and $M_S = -1$, removing the degeneracy of

Table 1. Relative Energies of the Six Lowest States Computed at the CASPT2+RASSI Levels (in cm^{-1}) and Contribution of the Two Lowest Spin-Free Triplets to These States

| state | energy | % triplet 1 | % triplet 2 |
|---------------|--------|-------------|-------------|
| 1 $ M_S = 1$ | 0.0 | 79.7 | 19.6 |
| 2 $ M_S = 1$ | 3.7 | 79.8 | 19.6 |
| 3 $M_S = 0$ | 246.0 | 98.3 | 0.0 |
| 4 $M_S = 0$ | 1178.7 | 0.0 | 98.1 |
| 5 $ M_S = 1$ | 1539.7 | 19.3 | 79.2 |
| 6 $ M_S = 1$ | 1557.7 | 19.3 | 79.7 |

the M_S components. Table 1 shows that the principal contribution to the first three states corresponds to the first spin-free triplet, although in the first two states, there is a noticeable contribution of the second triplet (see similar results at the CASSCF level in Table S3 in the Supporting Information, SI).

Taking into account that the spin–orbit coupling constant of the free nickel(II) ion is 644 cm^{-1} (and for complex **1** will be just slightly lower; see ref 14d), there is an interplay between the opposite effects, the first-order spin–orbit coupling and Jahn–Teller distortion, which have an energy influence of the same order of magnitude. Thus, we are in an intermediate situation between the two limits: predominance of the energy splitting of the Jahn–Teller effect or that corresponding to the first-order spin–orbit coupling. For this kind of situation, a complex Hamiltonian with a large number of parameters has been proposed.²¹ In order to keep a reasonable number of parameters in the theoretical and experimental analysis, we have considered only D and E ones. These ZFS parameters of **1** were accomplished using the procedure described by Chibotaru et al.¹⁹ The effective D and $|E|$ parameters obtained at the CASPT2+RASSI level were -244 and $|1.9|$ cm^{-1} , respectively (CASSCF values of -267 and $|1.3|$ cm^{-1}). The negative sign of D and its high value match well with the $|\Delta m_l| = 0$ transition between the two orbitals involved in the Jahn–Teller effect (d_{xy} and $d_{x^2-y^2}$ orbitals).⁵ Calculated g_x , g_y , and g_z values were 2.06, 2.09, and 3.41, respectively (CASSCF values 2.08, 2.11, and 3.50). On the other hand, for the complex previously reported by Borovik and co-workers, calculated D and $|E|$ parameters at the CASSCF level were -291 and $|0.04|$ cm^{-1} with a S value of 0.219, confirming that lower structural distortion enlarges the D value. It is worth mentioning that, with the same coordination mode, iron(II) (d^6 involving d_{xz} and d_{yz} orbitals; see Figure 1) and nickel(II) complexes exhibit negative D values, while equivalent cobalt(II) complexes (d^7 involving d_{xz} and $d_{x^2-y^2}$ orbitals and $|\Delta m_l| = 1$; see Figure 1) will present positive D parameters.⁵

SQUID studies show no alternating-current magnetic susceptibility signal, even applying an external dc field (as expected, see above). Magnetic susceptibility data were acquired from 2 to 300 K with an applied dc field of 0.7 T. Magnetization data were collected between 1.8 and 6.8 K at different applied magnetic fields (from 0.5 to 5 T). The shapes of the curves indicate the presence of a significant magnetic anisotropy (Figure S2, bottom).

Magnetization and susceptibility experimental data were fitted using the program *PHI*²² and the Hamiltonian shown in eq 3, which is divided into three terms; the first two terms are related to the crystal-field Hamiltonian (following the operator equivalent technique described by Stevens et al.),²³ where \hat{O}_k^q is the equivalent operator, and the last term is connected to the Zeeman Hamiltonian. We use the commonly employed

Hamiltonian to analyze magnetic data and obtain an estimation of the strong magnetic anisotropy with an effective D value despite the fact that for complex **1** there is in an intermediate situation where the energy splittings caused by the Jahn–Teller distortion and the first-order spin–orbit coupling are similar.

$$\hat{H} = \frac{D}{3}\hat{O}_2^0 + E\hat{O}_2^2 + \mu_B(g_x\hat{S}_x B_x + g_y\hat{S}_y B_y + g_z\hat{S}_z B_z) \quad (3)$$

Five parameters were selected to correlate the data: D , E , g_x , g_y , and g_z . Because of the high number of selected parameters, a good set of starting values is crucial because a different set of parameters could still reproduce the magnetic data. Because the experimental and simulated curves, using CASPT2, show a great agreement between them, the calculated values were employed as starting parameters for the fitting. From those, the values extracted for D ($|E|$) were -200 (1.7) cm^{-1} , with g_x , g_y , and g_z values of 2.67, 2.40, and 3.28, respectively. These results are in good agreement with the ones calculated by the CASPT2–RASSI method (Figure S2).

In order to check the stability and accuracy of the fitted values, the survey feature of the *PHI* code was employed. In general, a clear minimum can be found (in the residual plots, see the SI) corresponding to the smallest difference between the experimental and simulated curves. This minimum indicates the existence of a narrow range of values for each with the exception of the D parameter. Variation of D between -80 and -400 cm^{-1} results in the smallest residual values but with a small difference between them. Thus, we can conclude unambiguously that such a procedure leads to a large negative D value.

In conclusion, we have experimentally and theoretically studied a trigonal-pyramidal nickel(II) complex, showing a huge D value with excellent agreement between the experimental and calculated values. Being magnetic anisotropic, a fundamental property for the application of transition-metal complexes in data storage and quantum computing, this kind of system can be useful for such purposes either as isolated metal complexes or as building blocks.

■ ASSOCIATED CONTENT

■ Supporting Information

Crystallographic data (CIF format), synthesis and characterization of **1**, relative energies of the six lowest states at the CASSCF+RASSI level, and the fit procedure of the magnetic measurements. This material is available free of charge via the Internet at <http://pubs.acs.org>.

■ AUTHOR INFORMATION

■ Corresponding Author

*E-mail: silvia.gomez@qi.ub.es.

■ Notes

The authors declare no competing financial interest.

■ ACKNOWLEDGMENTS

The research was supported by the Spanish Ministerio de Economía y Competitividad (Grants CTQ2011-23862-C02-01 and CTQ2012-32247) and by Generalitat de Catalunya (Grant 2009SGR-1459). S.G.C. thanks the Spanish Ministerio de Educación, Cultura y Deporte for a predoctoral fellowship. The authors thankfully acknowledge the computer resources, technical expertise, and assistance provided by the Centro de Servicios Científicos y Académicos de Cataluña (CESCA).

■ REFERENCES

- Gatteschi, D.; Sessoli, R. *Angew. Chem., Int. Ed.* **2003**, *42*, 268.
- Aromí, G.; Aguilà, D.; Gamez, P.; Luis, F.; Roubeau, O. *Chem. Rev.* **2012**, *41*, 537.
- Freedman, D. E.; Harman, W. H.; Harris, T. D.; Long, G. J.; Chang, C. J.; Long, J. R. *J. Am. Chem. Soc.* **2010**, *132*, 1224.
- Cremades, E.; Ruiz, E. *Inorg. Chem.* **2011**, *50*, 4016.
- Gómez-Coca, S.; Cremades, E.; Aliaga-Alcalde, N.; Ruiz, E. *J. Am. Chem. Soc.* **2013**, *135*, 7010.
- Zadrozny, J. M.; Atanasov, M.; Bryan, A. M.; Lin, C.-Y.; Rekker, B. D.; Power, P. P.; Neese, F.; Long, J. R. *Chem. Sci.* **2013**, *4*, 125.
- (a) Lin, P.-H.; Smythe, N. C.; Gorelsky, S. I.; Maguire, S.; Henson, N. J.; Korobkov, I.; Scott, B. L.; Gordon, J. C.; Baker, R. T.; Murugesu, M. *J. Am. Chem. Soc.* **2011**, *133*, 15806. (b) Andres, H.; Bominaar, E. L.; Smith, J. M.; Eckert, N. A.; Holland, P. L.; Munck, E. *J. Am. Chem. Soc.* **2002**, *124*, 3012.
- Harman, W. H.; Harris, T. D.; Freedman, D. E.; Fong, H.; Chang, A.; Rinehart, J. D.; Ozarowski, A.; Sougrati, M. T.; Grandjean, F.; Long, G. J.; Long, J. R.; Chang, C. J. *J. Am. Chem. Soc.* **2010**, *132*, 18115.
- Weismann, D.; Sun, Y.; Lan, Y.; Wolmershaeuser, G.; Powell, A. K.; Sitzmann, H. *Chem.—Eur. J.* **2011**, *17*, 4700.
- (a) Zadrozny, J. M.; Long, J. R. *J. Am. Chem. Soc.* **2011**, *133*, 20732. (b) Zadrozny, J. M.; Liu, J.; Piro, N. A.; Chang, C. J.; Hill, S.; Long, J. R. *Chem. Commun.* **2012**, *48*, 3927. (c) Buchholz, A.; Eseola, A. O.; Plass, W. C. R. *Chim.* **2012**, *15*, 929. (d) Yang, F.; Zhou, Q.; Zhang, Y.; Zeng, G.; Li, G.; Shi, Z.; Wang, B.; Feng, S. *Chem. Commun.* **2013**, *49*, 5289.
- Jurca, T.; Farghal, A.; Lin, P.-H.; Korobkov, I.; Murugesu, M.; Richeson, D. S. *J. Am. Chem. Soc.* **2011**, *133*, 15814.
- Zhu, Y.-Y.; Cui, C.; Zhang, Y.-Q.; Jia, J.-H.; Guo, X.; Gao, C.; Qian, K.; Jiang, S.-D.; Wang, B.-W.; Wang, Z.-M.; Gao, S. *Chem. Sci.* **2013**, *4*, 1802.
- (11) Vallejo, J.; Castro, I.; Ruiz-García, R.; Cano, J.; Julve, M.; Lloret, F.; De Munno, G.; Wernsdorfer, W.; Pardo, E. *J. Am. Chem. Soc.* **2012**, *134*, 15704.
- (14) (a) Krzystek, J.; Park, J.-H.; Meisel, M. W.; Hitchman, M. A.; Stratemeier, H.; Brunel, L.-C.; Telsler, J. *Inorg. Chem.* **2002**, *41*, 4478. (b) Rogez, G.; Rebilly, J.-N.; Barra, A.-L.; Sorace, L.; Blondin, G.; Kirchner, N.; Duran, M.; van Slageren, J.; Parsons, S.; Ricard, L.; Marvilliers, A.; Mallah, T. *Angew. Chem., Int. Ed.* **2005**, *44*, 1876. (c) Ruamps, R.; Batchelor, L. J.; Maurice, R.; Gogoi, N.; Jiménez-Lozano, P.; Guihéry, N.; de Graaf, C.; Barra, A.-L.; Sutter, J.-P.; Mallah, T. *Chem.—Eur. J.* **2013**, *19*, 950. (d) Ruamps, R.; Maurice, R.; Batchelor, L.; Boggio-Pasqua, M.; Guillot, R.; Barra, A. L.; Liu, J.; Bendeif, E.-E.; Pillet, S. b.; Hill, S.; Mallah, T.; Guihéry, N. *J. Am. Chem. Soc.* **2013**, *135*, 3017.
- (15) (a) Bersuker, I. B. *The Jahn–Teller effect*; Cambridge University Press: Cambridge, U.K., 2006; p 52. (b) Bersuker, I. B. *Electronic Structure and Properties of Transition Metal Compounds: Introduction to the Theory*; John Wiley & Sons, Inc.: Hoboken, NJ, 2010; p 351.
- (16) Allen, F. H. *Acta Crystallogr., Sect. B: Struct. Sci.* **2002**, *58*, 380.
- (17) (a) Alvarez, S.; Alemany, P.; Casanova, D.; Cirera, J.; Llunell, M.; Avnir, D. *Coord. Chem. Rev.* **2005**, *249*, 1693. (b) Llunell, M.; Casanova, D.; Cirera, J.; Alemany, P.; Alvarez, S. *Shape program*, version 2; Universitat de Barcelona: Barcelona, Spain, 2010.
- (18) Ray, M.; Yap, G. P. A.; Rheingold, A. L.; Borovik, A. S. *J. Chem. Soc., Chem. Commun.* **1995**, 1777.
- (19) Chibotaru, L. F.; Ungur, L. *J. Chem. Phys.* **2012**, *137*, 064122.
- (20) Aquilante, F.; De Vico, L.; Ferré, N.; Ghigo, G.; Malmqvist, P.-A.; Neogrády, P.; Pedersen, T. B.; Pitonák, M.; Reiher, M.; Roos, B. O.; Serrano-Andrés, L.; Urban, M.; Veryazov, V.; Lindh, R. *J. Comput. Chem.* **2010**, *31*, 224.
- (21) Atanasov, M.; Ganyushin, D.; Pantazis, D. A.; Sivalingam, K.; Neese, F. *Inorg. Chem.* **2011**, *50*, 7460.
- (22) Chilton, N. F.; Anderson, R. P.; Turner, L. D.; Soncini, A.; Murray, K. S. *J. Comput. Chem.* **2013**, *34*, 1164.
- (23) Abragam, A.; Bleaney, B. *Electron Paramagnetic Resonance of Transition Ions*; Oxford University Press: Oxford, U.K., 1970.